

Two-Step Four-Electron Reduction of Molecular Oxygen at Iodine-Adatoms-Modified Gold Electrode in Alkaline Media

Md. Rezwana Miah¹ and Takeo Ohsaka^{*}

Department of Electronic Chemistry, Interdisciplinary Graduate School of Science and Engineering, Tokyo Institute of Technology, 4259 Nagatsuta, Midori-ku, Yokohama 226-8502, Japan

*E-mail: ohsaka@echem.titech.ac.jp

Received: 21 October 2011 / Accepted: 3 December 2011 / Published: 1 January 2012

The effect of in situ reversible adsorption / desorption of iodide / iodine-adatoms at polycrystalline gold (Au) electrode on the oxygen reduction reaction (ORR) was studied in alkaline media using cyclic voltammetric technique. The ORR was completely inhibited by the compact iodine-adatoms at more positive potential than ca. -0.25 V vs. Ag / AgCl / NaCl (sat.). The ORR commences simultaneously with the potential-induced reductive desorption of the iodine-adatoms. The interesting feature observed is the complete inhibition of the heterogeneous catalytic disproportionation reaction of the electrogenerated HO_2^- to O_2 and OH^- by the iodine-adatoms chemisorbed at the Au electrode surface. Consequently, compared with the bare Au electrode, a decrease in the first cathodic peak current as well as a large increase (ca. 12 times) of the second consecutive cathodic peak current corresponding to the further reduction of HO_2^- to OH^- , that is, the two-step four-electron ORR was observed at the iodine-adatoms-modified Au electrode in alkaline media. Effect of the other halides, e.g., bromide, chloride and fluoride was also studied.

Keywords: Chemisorption; Iodine-adatoms; Oxygen reduction reaction; Two-step four-electron ORR; Disproportionation

1. INTRODUCTION

Oxygen reduction reaction (ORR) is of great importance for the electrochemical energy conversion in fuel cells and metal-air batteries, corrosion and some other industrial processes [1-6]. However, it continues to be a challenge to explore the mechanism / pathway of the ORR because of its complex kinetics as well as to find out cheaper electrocatalysts that could support the desired four-electron reduction process being vitally important for the efficient performance of the fuel cells. The mechanism of the ORR is highly sensitive to the type of electrode materials, their surface structures,

surface modifiers and the nature of the electrolytic solutions. For example, our group has reported that polycrystalline gold (Au) electrodes modified by cysteine and iodine-adsorbed submonolayers, interestingly, show a quasi-reversible ORR although this reaction is fully irreversible at the clean Au electrode in the same media [7,8]. We have also reported that a well-defined inverted peak is observed at lead-modified Au electrode during the ORR in alkaline solution when it contains an appropriate amount of iodide [9]. Effect of bromide-adsorbed on the ORR was investigated by Adzic et al. [10-12] and Markovic et al. [13] in bromide-containing electrolytes of relatively lower pH using various single crystalline metallic electrodes. Those studies demonstrated that bromine-adsorbed on the electrode surface inhibit the ORR to a variable extent: An ordered compact bromine-adsorbed layer results in a complete inhibition of the ORR, while a partial inhibition occurs depending on the potential-dependent surface coverage of the bromine-adsorbed and the electrode materials. H_2O_2 is often produced as an intermediate in the ORR. We have reported that iodine-adsorbed show very unique effect on the reduction of HO_2^- in alkaline media [14]. The cyclic voltammetric behavior of HO_2^- at the clean Au electrode in alkaline media is very complicated because of several simultaneously occurring chemical and electrochemical processes, namely, heterogeneous disproportionation of HO_2^- to O_2 and electrochemical oxidation of HO_2^- to O_2 , electroreduction of the produced O_2 to HO_2^- and electroreduction of HO_2^- to OH^- [14]. Our previous study showed that in situ fabrication of compact iodine-adsorbed effectively inhibits all other processes other than only a quantitative electroreduction of HO_2^- to OH^- at the Au electrode surface freshly generated by the potential-induced desorption of the iodine-adsorbed [14].

Chemisorption of halides, especially iodide at different metallic electrodes has become a subject of extensive studies being significantly important in a wide range of electrochemical applications [14-30]. Therefore, chemisorption of iodide and evaluation of its adsorbed layer structures have been extensively studied using a wide range of in situ and ex situ techniques, namely, electrochemical analyzer [14], low energy electron diffraction (LEED), Auger electron spectroscopy (AES) and X-ray photoelectron spectroscopy (XPS) [31,32], surface enhanced Raman scattering (SERS) [33], scanning tunneling microscopy (STM) [34-41], atomic force microscopy (AFM) [42], surface X-ray scattering (SXS) [43,44], electrochemical quartz crystal microbalance (ECQM) [45,46].

In the present study, we address the effect of the in situ fabricated iodine-adsorbed at the Au electrode on the pathway of the ORR in alkaline media using cyclic voltammetric technique. Effect of other halides, such as bromide, chloride and fluoride on the ORR was also studied.

2. EXPERIMENTAL

For cyclic voltammetric measurements, Au electrodes with ($\phi = 1.6$ mm sealed in a Teflon tube) an exposed surface area of 2.01×10^{-2} cm^2 were used as working electrodes. A spiral Pt wire and an Ag /AgCl / NaCl (sat.) were the counter and reference electrodes, respectively. A conventional two-compartment Pyrex glass cell was used. Prior to measurements N_2 or O_2 gas was bubbled into the cell solution for 30 min to obtain N_2 - or O_2 -saturated solution. Commercially available H_2O_2 was

purchased and stored in low temperature and used as received. All the measurements were performed at 25 ± 1 °C. The Au electrodes were polished with aqueous slurries of successively finer alumina powder (down to $0.06 \mu\text{m}$) and were sonicated for 10 min in Milli-Q water. The Au electrodes were then electrochemically pretreated in 0.05 M H_2SO_4 solution by repeating the potential scan in the range of -0.2 to 1.5 V vs. Ag / AgCl / NaCl (sat.) at 0.1 V s^{-1} for 10 min or until the cyclic voltammetric characteristic of a clean Au electrode was obtained. A roughness factor (rf) of 1.2 was estimated for the Au electrodes as calculated from the charge passed during the formation of the surface oxide monolayer [47]. The ORR was carried out in O_2 -saturated 0.1 M NaOH solution containing 12.5 mM of potassium iodide (KI). For the ex situ modification, the Au electrode was soaked in 0.1 M NaOH aqueous solution containing 0.5 M of KI for 10 min and washed thoroughly with milli-Q water before its use. The ORR was also investigated in O_2 -saturated 0.1 M NaOH solutions containing 12.5 mM of potassium bromide (KBr), potassium chloride (KCl) and potassium fluoride (KF) separately. The electrodes modified with halide-adlayer are hereinafter denoted as the $\text{X}_{(\text{ads})} | \text{Au}$ electrode, where $\text{X}_{(\text{ads})}$ stands for $\text{I}_{(\text{ads})}$, $\text{Br}_{(\text{ads})}$, $\text{Cl}_{(\text{ads})}$ or $\text{F}_{(\text{ads})}$. Electrochemical measurements were performed using an ALS CHI-832A electrochemical analyzer.

3. RESULTS AND DISCUSSION

3.1. Chemisorption of iodide at the Au electrode

Iodide undergoes a rapid oxidative chemisorption on the Au electrode surface forming a monolayer of atomic iodine-adatoms. The details in this regard have been presented in our earlier study [14] as well as in the studies by other groups [32,41,48-50]. According to those studies, the surface coverage and adlayer structures of the iodine-adatoms are largely influenced by the applied potential in the iodide-containing solution. In brief, at potential more positive than ca. -0.2 V vs. Ag / AgCl / NaCl (sat.) in alkaline solution, iodine-adatoms undergo a unidirectional compression as the electrode potential becomes more and more positive, resulting in a continuous increase of the surface coverage of iodine leading to the formation of a close-packed rotated-hexagonal adlayer structure. Such a unidirectional compression of iodine-adatoms is well-known in literatures as “electrocompression” [14,40,49,50]. The thus-formed compact iodine-adlayer may effectively inhibit the inner-sphere electron transfer process [14], while it may significantly increase the electrode response of many outer-sphere electron transfer reactions [51,52]. At potential below -0.2 V, potential-induced continuous desorption of iodine leads to the conversion of the close-packed rotated-hexagonal structure into a relatively less-packed rectangular adlayer structure [10]. Electrochemical reactions may then take place at the bare fraction of the electrode surface [7,8]. As the potential is swept to more negative value, the surface coverage of the iodine-adatoms decreases significantly. At potential ca. -1.0 V vs. Ag / AgCl / NaCl (sat.) the iodine-adatoms are almost completely desorbed in alkaline solution and inner-sphere electron transfer reaction may then take place at the thus-generated fresh bare surface of the electrode [14]. As the potential is swept back to the positive direction, the specific adsorption of iodide begins [14,32,48] and the surface coverage of iodine-adlayer increases

with increasing potential. Therefore, iodide adsorption / desorption is a reversible process and its surface coverage and adlayer structures can suitably be controlled electrochemically for a desired chemical / electrochemical purpose.

3.2. Reduction of O_2 at the $I_{(ads)} / Au$ electrode

Fig. 1 shows the CVs obtained at the Au electrode in (a,b) N_2 - and (a',b') O_2 -saturated 0.1 M NaOH solution containing (a,a') 0.0 and (b,b') 12.5 mM KI.

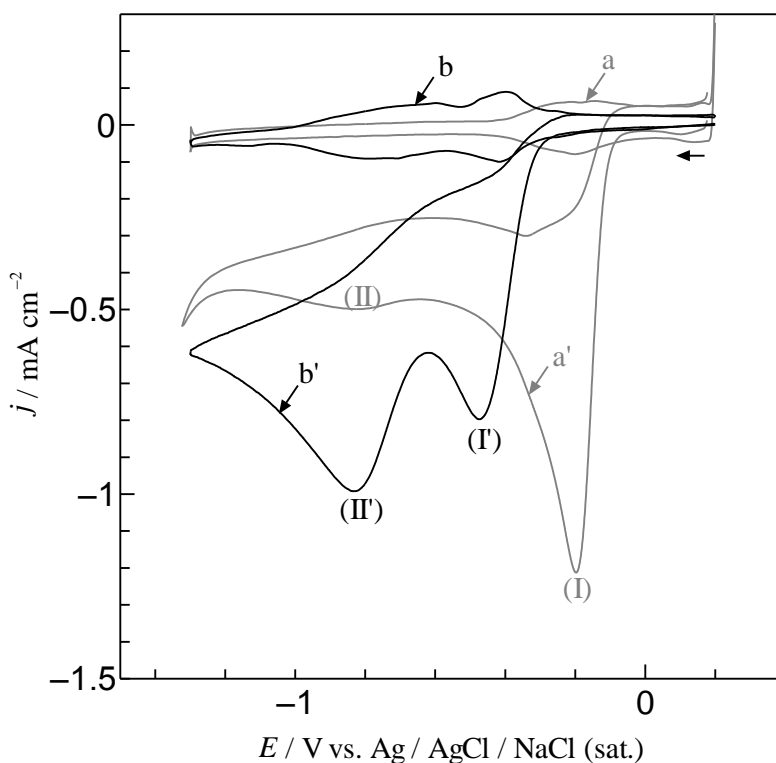
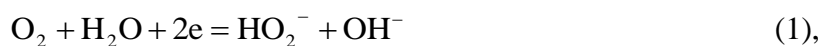


Figure 1. CVs obtained at the Au electrode in (a,b) N_2 - and (a',b') O_2 -saturated 0.1 M NaOH solution containing (a,a') 0.0 and (b,b') 12.5 mM KI. Electrode was held in the solution for 10 min before measuring the CVs (b) and (b'). Potential scan rate: 0.1 V s^{-1} .

Both of the electrodes, e.g., the Au and $I_{(ads)} / Au$ electrodes exhibit two cathodic peaks [assigned as (I) and (II) for the Au electrode and (I') and (II') for the $I_{(ads)} / Au$ electrode] in O_2 -saturated solutions. The shape of the CV obtained at the $I_{(ads)} / Au$ electrode (curve b') is comparable to the reported data on the ORR at the Au (111) single crystalline electrode in alkaline media by Kongkanand et al. [53]. It is well-known that the first peak (I) appearing at relatively positive potential is assigned to the formation of HO_2^- according to the reaction (1)



,while the second consecutive peak (II) appearing at relatively lower potential is assigned to the further reduction of the electrogenerated HO_2^- according to the reaction (2) [53,54]:



Similarly to the bare Au electrode, the peaks (I') and (II') appearing at the $\text{I}_{(\text{ads})} | \text{Au}$ electrode are also attributed to the same reactions (1) and (2), respectively. However, the remarkable features observed at the $\text{I}_{(\text{ads})} | \text{Au}$ electrode compared to the bare Au electrode are: (i) the peak (I') appears at -0.49 V, which is ca. 0.29 V more negative and its intensity decreases by ca. 33% and (ii) the second consecutive reduction peak (II') assigned to the further reduction of the HO_2^- electrogenerated in peak (I') potential region increases by ca. 12 times. The interesting feature, therefore, observed in the present study is that the peak (II') current increases remarkably as compared with the peak (II) which implies that the ORR pathway at the $\text{I}_{(\text{ads})} | \text{Au}$ electrode could be altered from that at the bare Au electrode by the in situ formation of the iodine-adatoms.

The onset potential (ca. -0.25 V) for the ORR at the $\text{I}_{(\text{ads})} | \text{Au}$ electrode is 210 mV more negative as compared with the bare Au electrode (compare curves a' and b'), because of the blocking of the access of O_2 molecules to the electrode surface by the highly ordered and compact iodine-adlayer as we have discussed in the preceding section [14]. The ORR is an inner-sphere electron transfer process and hence the reaction cannot proceed until some vacant sites are generated on the Au electrode surface for the access of the O_2 molecules. Below -0.25 V, the iodine-adlayer begins to undergo potential-induced partial reductive desorption from the Au electrode surface and thus the close-packed rotated hexagonal structure is converted to a relatively less-packed structure with defects and holes in the structure [14]. Therefore, the peak (I') is in fact assigned to two superimposed processes, namely, (i) the partial desorption of the iodine-adatoms and (ii) the access of O_2 molecules to the electrode surface through the vacant sites and its electroreduction forming HO_2^- . More over, the adsorption efficiency of O_2 molecules (which is vitally important for the initiation of the ORR) at the $\text{I}_{(\text{ads})} | \text{Au}$ electrode could be decreased by the existing iodine-adatoms, which is a very strong adsorbate for the Au electrode surface. Therefore, the ORR at the $\text{I}_{(\text{ads})} | \text{Au}$ electrode requires a higher overpotential than the bare Au electrode.

The decrease of this peak (I') current (by ca. 33%) apparently could be attributed to (i) the less accessible surface area at the $\text{I}_{(\text{ads})} | \text{Au}$ electrode, (ii) the inhibition of the catalytic decomposition of the produced HO_2^- to O_2 and OH^- by the iodine-adatoms and (iii) the hydrophobic nature of the iodine-adatoms. A considerable amount of the iodine-adatoms still remain adsorbed at the peak (I') potential region. We demonstrated in our previous article [14] that the surface coverages of the iodine-adatoms at 0 (at which the compact monolayer is formed) and -0.49 V vs. Ag / AgCl / NaCl (sat.) in alkaline media are 1.54×10^{15} and 1.02×10^{15} atoms cm^{-2} , respectively. Therefore, approximately 66% of the total surface area of the Au electrode is still covered by the iodine-adatoms at -0.49 V. The ORR in the peak (I') takes place at the numerous micro-arrays of the vacant sites, i.e., the Au (111) facets (explained later) of the $\text{I}_{(\text{ads})} | \text{Au}$ electrode (7,8). The diffusion layer of O_2 molecules at a given vacant site may overlap with those at the neighboring vacant sites and the whole of the electrode

surface thus can practically be effective for the ORR, therefore suggesting that the less accessible surface area at the $I_{(ads)}|Au$ electrode may not have a significant role in the less peak (I') current intensity. The clean Au electrode surface is well-known to catalytically decompose HO_2^- in alkaline media to produce O_2 and OH^- [7,8,14]. The HO_2^- produced in the ORR at the bare Au electrode in the peak (I) potential region, therefore, undergoes the disproportionation reaction according to reaction (3) [7,8,14]:



The reaction (3) increases the surface concentration of O_2 and thus increases the peak (I) current intensity for the ORR at the bare Au electrode (7,8,14). On the contrary, at the $I_{(ads)}|Au$ electrode, the reduction of O_2 to HO_2^- in the peak (I') region mainly occurs at the Au (111) domains of the Au electrode. Previous reports by our group on the potential-induced desorption of various thiols and iodide [7,8,55] and reports by other groups on the desorption of cyanide [56] and iodide [57] using the Au and single crystalline Au (111), Au (100) and Au (110) electrodes reveal that the binding strength between adsorbates and the Au facets is of the following order: Au (110) > Au (100) > Au (111). Therefore, the iodine-adatoms preferably undergo potential-induced (i.e., reductive) desorption from the Au (111) facets of the Au electrode surface and the ORR in the peak (I') potential region occurs at the thus-formed free Au (111) facets. The Au (111) facets of the Au electrode surface are noncatalytic towards the disproportionation reaction of HO_2^- to O_2 and OH^- (i.e., the reaction (3)) [7,8,58]. In addition, the remaining iodine-adatoms also poison the catalytic activity of the Au electrode for the disproportionation of HO_2^- . Therefore, unlike the bare Au electrode, the electrogenerated HO_2^- in the peak (I') potential region is highly stable and hence the reaction (3) no longer takes place at the $I_{(ads)}|Au$ electrode. The less surface concentration of O_2 , therefore, consequently results in the lower peak (I') current as compared to the peak (I) current. Hence, the efficient inhibition of the catalytic decomposition of the electrogenerated HO_2^- to O_2 and OH^- could be considered as the principal reason for the decreased peak (I') current observed at the $I_{(ads)}|Au$ electrode. The hydrophobic nature of the iodine-adlayer may also be a minor reason for the less intense peak (I') current for the ORR in the case of the $I_{(ads)}|Au$ electrode.

The peak (II') height is increased by ca. 12 times at the $I_{(ads)}|Au$ electrode compared with the peak (II) at the bare Au electrode. The peak (II') height is considered to be almost equal to the peak (I') height, although these heights are not precisely determined because a proper current baseline for the peak (II') cannot be obtained experimentally. The ability of the $I_{(ads)}|Au$ electrode to enhance the peak (II') current is mainly attributed to the inhibition of the heterogeneous catalytic decomposition of the produced HO_2^- as discussed earlier [7,8,14]. The electrogenerated HO_2^- , therefore, without undergoing its disproportionation reaction, remains at the vicinity of the electrode surface and its reduction takes place at the freshly generated Au electrode surface in the peak (II') potential region. The details on the electroreduction of HO_2^- at the iodine-adatoms-modified Au electrode in alkaline media have been presented in our previous report [14].

3.3. Effect of added H_2O_2 into the solution

The two-step four-electron ORR was further demonstrated by performing experiments in the presence of added HO_2^- . Fig. 2 shows the CVs obtained at the Au electrode in (a,b) O_2 - and (c) N_2 -saturated 0.1 M NaOH solution containing 12.5 mM KI and (a) 0.0 and (b,c) 10 mM H_2O_2 .

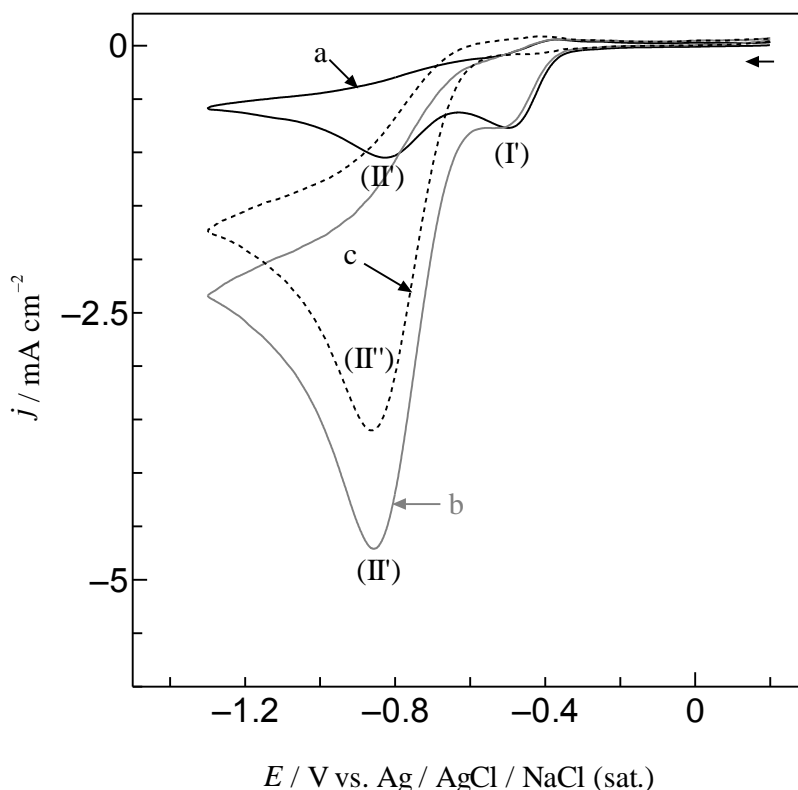


Figure 2. CVs obtained at the Au electrode in (a,b) O_2 - and (c) N_2 -saturated 0.1 M NaOH solution containing 12.5 mM KI and (a) 0.0 and (b,c) 10 mM H_2O_2 . Potential scan rate: 0.1 V s^{-1} .

The notable features observed at the $\text{I}_{(\text{ads})} | \text{Au}$ electrode in the presence of the added H_2O_2 are (i) the peak (I') current in O_2 -saturated solution remained unchanged (compare curves a and b), (ii) the second consecutive peak (II') current increased remarkably compared to that obtained in O_2 -saturated solution in the absence of the added HO_2^- and (iii) in N_2 -saturated solution, the peak (I') current completely disappeared and a well-defined peak [assigned as (II'')] current was observed at the same potential as the peak (II') potential (curve c). Similar voltammetric behaviors of the ORR in the presence of H_2O_2 were reported by our group using electrodeposited gold nanoparticles-modified Au electrode in acidic media [54]. The unchanged peak (I') current in O_2 -saturated solution signifies two things: (i) HO_2^- does not undergo reduction at the peak (I') potential region and (ii) HO_2^- is not catalytically decomposed to O_2 by the $\text{I}_{(\text{ads})} | \text{Au}$ electrode. Decomposition of HO_2^- to O_2 should result in an increase of the surface concentration of O_2 and thus increase the peak (I') current. Therefore, peak (I') in curve (a) is obviously assigned to the two-electron reduction of O_2 forming stable HO_2^- .

The second consecutive peak (II') current is increased due to the reduction of the added HO_2^- along with the reduction of the HO_2^- electrogenerated in the peak (I') potential region [54]. The intensity of the peak (II'') current (curve c) is less as compared with the peak (II') current (curve b) because only the added HO_2^- undergoes reduction in the N_2 -saturated solution. Appearance of the peak (II'') obviously suggests that the HO_2^- electrogenerated in the peak (I') region undergoes reduction in the peak (II') potential region (curve a). The sum of the peak (II') and (II'') currents of curves (a) and (c), respectively, is equal to the peak (II') current of curve (b), implying that the added and electrogenerated HO_2^- can undergo reduction without a significant catalytic decomposition at the electrode surface. These observations in the presence of the added HO_2^- , therefore, obviously demonstrate the two-step four-electron ORR at the $\text{I}_{(\text{ads})} | \text{Au}$ electrode in alkaline media.

3.4. Effect of scan rate on the ORR

The ORR was investigated at the $\text{I}_{(\text{ads})} | \text{Au}$ (poly) electrode in the potential scan rate range of 0.005 to 1.0 V s^{-1} (Fig. 3).

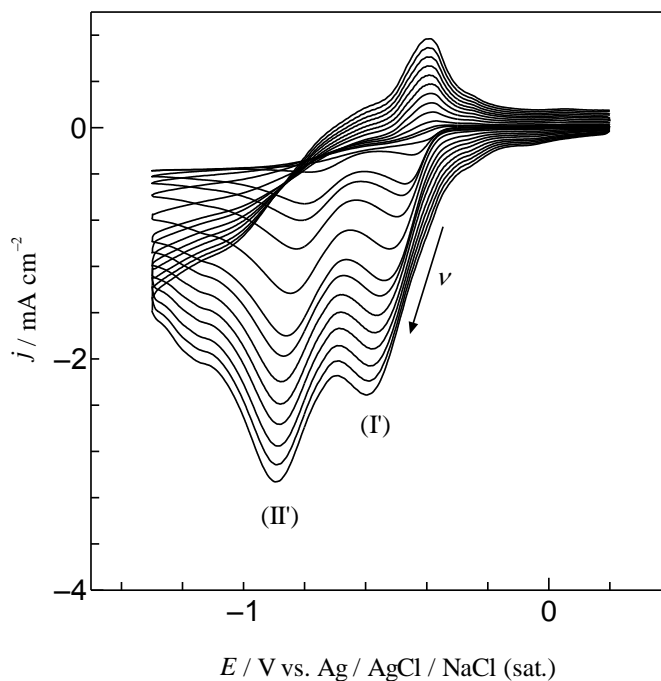


Figure 3. CVs obtained at the Au electrode in O_2 -saturated 0.1 M KOH solution containing 12.5 mM KI at various scan rates: 0.005, 0.03, 0.05, 0.1, 0.2, 0.3, 0.4, 0.5, 0.6, 0.7, 0.8, 0.9 and 1.0 V s^{-1} (from top to bottom).

The peak (I') current was determined from the CVs shown in Fig. 3 and plotted (after the background correction) as a function of the square root of scan rate ($v^{1/2}$). Fig. 4 shows that the values

of the peak current nicely ($r^2 = 0.998$) fall on a straight line passing through the origin, indicating that the ORR is solely controlled by the diffusion of O_2 molecules to the electrode surface.

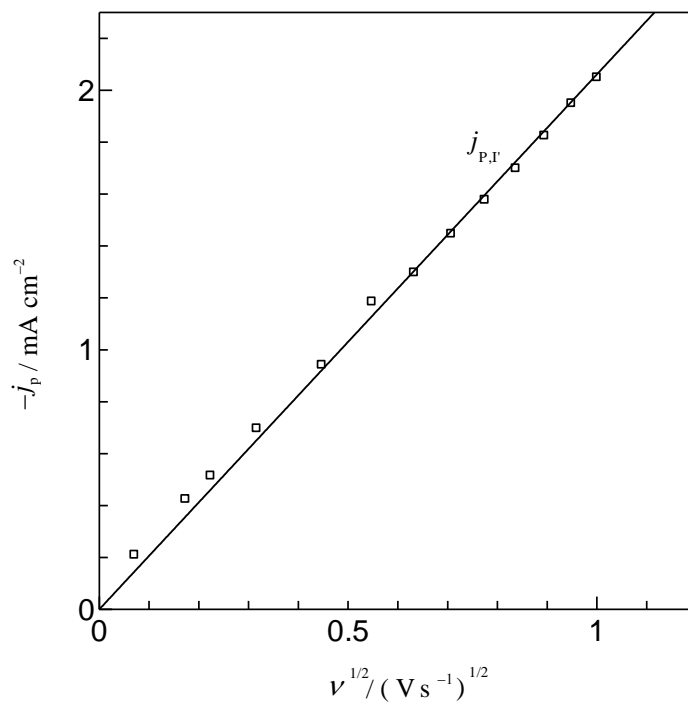


Figure 4. Linear plot of the first peak (I) current vs. the square root of scan rate for the ORR at the $I_{(ads)} | Au$ electrode. Data were taken from Fig. 3.

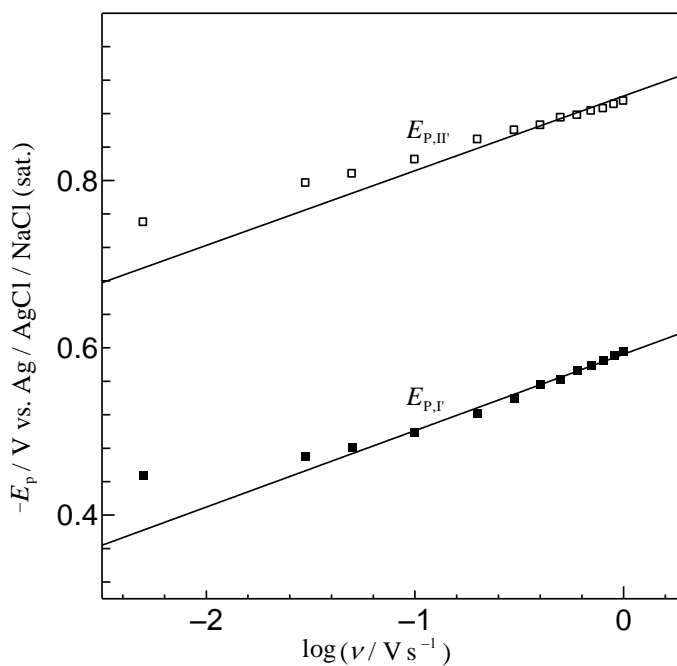


Figure 5. Linear plots of the first (I) and second (II) peak potentials vs. logarithm of the scan rate ($\log \nu$). Data were taken from Fig. 3.

The plot of the peak (II') current vs. $\nu^{1/2}$ was excluded as the height of the peak (II') current could not be estimated precisely owing to the lack of a well-defined current baseline. On the other hand, at the bare Au electrode the peak (I) current was not proportional to $\nu^{1/2}$ and the peak (II) current diminished quickly with increasing ν (not shown). The peak (I') and (II') potentials ($E_{P,I'}$ and $E_{P,II'}$) were also derived from the CVs shown in Fig. 3 and plotted as a function of $\log \nu$. Fig. 5 shows that the values of $E_{P,I'}$ and $E_{P,II'}$ fall on their individual straight lines at relatively higher scan rates. The slopes of both straight lines are comparable and approximately equal to ca. -9.14×10^{-2} V decade $^{-1}$, from which the cathodic transfer coefficients (α_c) were found to be 0.33 for both the reduction of O_2 to HO_2^- and further reduction of HO_2^- to OH^- .

3.5. Effect of surface overage of the iodine-adatoms on the ORR

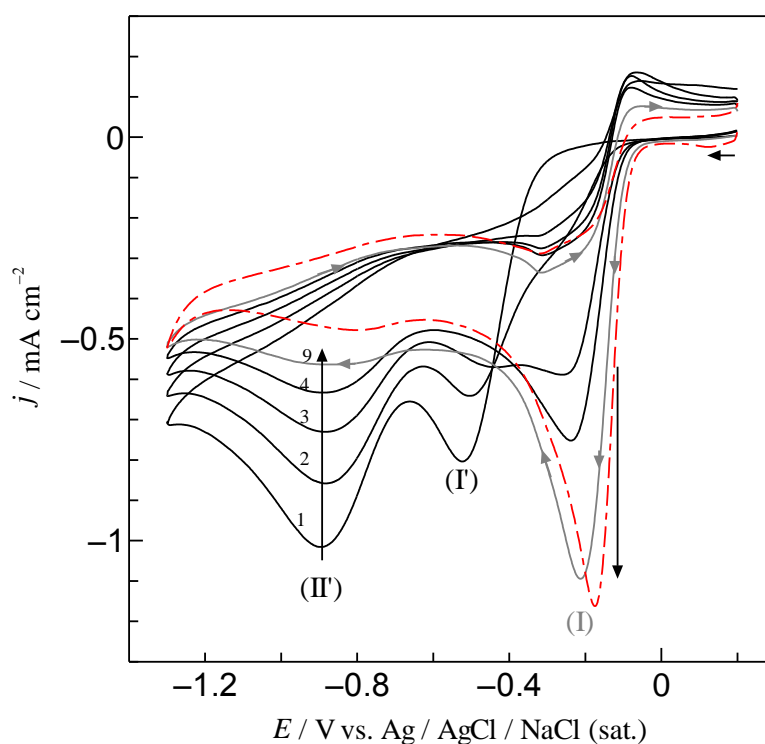


Figure 6. CVs obtained at the $I_{(ads)} | Au$ electrode in O_2 -saturated 0.1 M NaOH solution containing no added iodide at the 1st (1), 2nd (2), 3rd (3), 4th (4) and 9th (9) cycle. The $I_{(ads)} | Au$ electrode was prepared by soaking the Au electrode in 0.1 M NaOH solution containing 0.5 M KI for 10 min. The dot 2-dashed line shows the CV obtained at the bare Au electrode in the same media. Potential scan rate: 0.1 V s^{-1} .

The bare Au electrode was ex situ coated with a monolayer of spontaneously formed iodine-adatoms by soaking the electrode in 0.1 M NaOH solution containing 0.5 M KI for 10 min under open circuit condition. The thus-fabricated $I_{(ads)} | Au$ electrode was then transferred into O_2 -saturated 0.1 M NaOH solution containing no iodide ion and the ORR was investigated with continuous potential scan cycling. Fig. 6 clearly shows that the peak (I') and (II') currents diminish quickly and the peak (I)

grows rapidly with potential scan cycling. CV obtained at the 9th cycle is almost similar to that obtained at the bare Au electrode. As a result of the continuous potential scan cycling in the iodide free solution, the iodine-adatoms undergo potential-induced reductive desorption from the electrode surface in the cathodic sweep and the resulting iodide ions diffuse into the bulk of the solution. Consequently, the surface coverage of the iodine-adatoms decreases gradually and thus the CV characteristic of the ORR obtained at the bare Au electrode was observed in the 9th cycle, in which the surface is actually free of the iodine-adatoms. The minor oxidation peak current appearing at ca. -0.05 V at the $I_{(ads)}$ | Au electrode is attributed to the oxidation of HO_2^- to O_2 [8,59,60]. Therefore, the iodine-adlayer can exist on the electrode surface only when the solution contains iodide ions and play a significant role in the two-step four-electron ORR.

3.6. The ORR at the other halides-modified Au electrodes

For comparison, the ORR was also investigated at the Au electrode in O_2 -saturated 0.1 M NaOH solution containing 12.5 mM of KBr, KCl or KF and the results are presented in Fig. 7. Fluoride did not show any effect on the ORR as it does not undergo adsorption at the Au electrode surface and hence the data is not shown for simplicity. Chloride exhibits only a little effect on the ORR at the Au electrode.

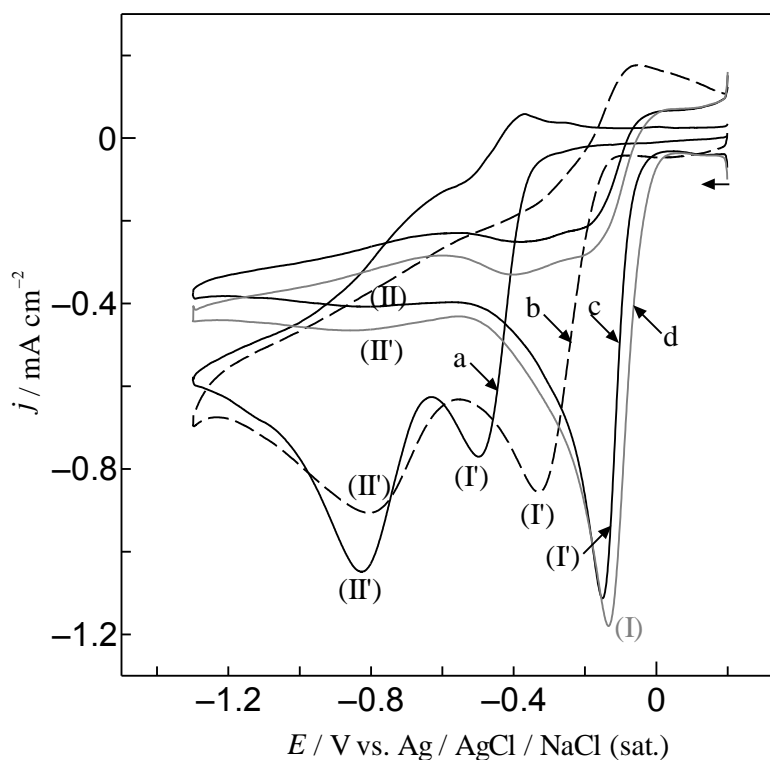


Figure 7. CVs obtained at the Au electrode in O_2 -saturated 0.1 M NaOH solution containing 12.5 mM of (a) KI, (b) KBr or (c) KCl. Electrode was held in each solution for 30 min before measurements. CV (d) was obtained at the bare Au electrode in the absence of the halides. Potential scan rate: 0.1 V s^{-1} .

Holding the Au electrode for 30 min in 0.1 M NaOH solution containing 12.5 mM KCl resulted in a decrease of the peak (I') current only by ca. 5% and a shift of the peak potential to the negative direction by 6 mV, while the peak (II') current and potential remained almost unchanged (compare curves c and d). The results imply that the adsorption affinity of chloride at the Au electrode surface in alkaline media is considerably low as compared with iodide. Bromide shows an intermediate effect between iodide and chloride implying that bromide has a moderate adsorption affinity on the Au electrode in alkaline media. In the presence of bromide, the peak (II') potential remains almost similar to that in the presence of iodide and chloride. However, the peak (I') appears at -0.33 V which is 0.16 V more positive compared to that in the presence of iodide (compare curves a and b) and 0.18 V more negative compared to that in the presence of chloride (compare curves b and c). The notable effect observed in the presence of bromide is the decrease of the peak (II') current by ca. 33% and the increase of the peak (I') by ca. 6% compared to the iodide-containing solution. The decrease of the peak (II') current may be due to the fact that the bromine-adlayer may not be fully efficient for the inhibition of the disproportionation reaction of the electrogenerated HO_2^- . The shift of the peak (I') potential to the positive direction implies that the potential-induced reductive desorption of the bromine-adlayer takes place at more positive potential than the iodine-adlayer, that is, the binding strength between the bromine-adatoms and the Au electrode surface is less than the corresponding strength of the iodine-adatoms. A little increase of the peak (I') current may be correlated to (i) the larger accessible surface area (as bromide does not undergo strong adsorption and form a full monolayer [59]) and (ii) the probable disproportionation of the minute amount of the electrogenerated HO_2^- to O_2 and OH^- , which increase the surface concentration of O_2 . The unique feature obtained at the $\text{Br}_{(\text{ads})} | \text{Au}$ electrode is the appearance of an oxidation peak current at ca. -0.05 V which is assigned to the oxidation of HO_2^- to O_2 at the bare fraction of the Au electrode surface. It is to be noted that a close-packed halide-adlayer at the Au electrode completely inhibits the oxidation of HO_2^- [14]. This feature implies that unlike the iodide-containing solution, the surface is not completely blocked by the bromine-adatoms during the anodic potential scan in the bromide-containing solution because of the less adsorption affinity of bromide as compared with iodide. The details on the in situ formation of the bromine-adatoms on the Au electrode surface in alkaline solution, its surface coverage and the effect of the adatoms on the electrochemical oxidation of HO_2^- have been presented in our earlier report [59]. In summary, it can be concluded that the poisoning effect of the halide-adatoms on the catalytic activity of the Au electrode surface towards the disproportionation of the electrogenerated HO_2^- to O_2 and OH^- decreases in the order of $\text{I}_{(\text{ads})} > \text{Br}_{(\text{ads})} > \text{Cl}_{(\text{ads})}$. The two-step four-electron ORR thus takes place almost ideally at the $\text{I}_{(\text{ads})} | \text{Au}$ electrode, but it becomes less ideal at the $\text{Br}_{(\text{ads})} | \text{Au}$ electrode and much less ideal at the $\text{Cl}_{(\text{ads})} | \text{Au}$ electrode.

4. CONCLUSIONS

The ORR was investigated at the iodine-adatoms-modified Au electrode in O_2 -saturated 0.1 M NaOH solution in the presence of iodide. The ORR was completely inhibited by a close-packed iodine-

adlayer existing at the Au electrode surface at more positive potential than ca. -0.25 V. The ORR appears as a superimposed reaction with the potential-induced reductive desorption of the iodine-adatoms. The unique feature observed in the study is the electrogeneration of stable HO_2^- at the $\text{I}_{(\text{ads})}|\text{Au}$ electrode in the first peak potential (-0.49 V) region owing to the complete inhibition of the disproportionation reaction of HO_2^- to O_2 by the iodine-adatoms chemisorbed at the electrode surface. The second consecutive peak current appearing at ca. -0.83 V corresponding to the further reduction of the electrogenerated HO_2^- to OH^- was thus increased by ca. 12 times. The two-step four-electron ORR is a well-known phenomenon, but the electrogeneration of HO_2^- as a stable intermediate at metallic electrodes is hardly observed because of its rapid disproportionation reaction, which is very promptly catalyzed by the electrode surfaces themselves. The in situ electrogeneration of stable HO_2^- using the $\text{I}_{(\text{ads})}|\text{Au}$ electrode could be useful in many electrochemical and chemical processes. Bromide is less efficient adsorbate than iodide to inhibit the disproportionation of HO_2^- , while chloride has no significant role in this regard. Hydrodynamic studies are currently undertaken to further clarify the two-step four-electron ORR at the iodine-adatoms-modified Au electrode and will be reported soon elsewhere.

ACKNOWLEDGEMENTS

The present work was supported by the Grant-in-Aids for Scientific Research on Priority Areas (No.417), Scientific Research (No. 12875164), and Scientific Research (A) (No. 10305064) to T. Ohsaka, from the Ministry of Education, Culture, Sports, Science and Technology, Japan (MEXT) and also from the New Energy and Industrial Technology Development Organization (NEDO), Japan. Dr. Md. Rezwan Miah thanks the Government of Japan for a MEXT scholarship.

References

1. R. Adzic, A. Tripkovic and R. Atanasoski, *J. Electroanal. Chem.* 94 (1978) 231.
2. M.S. El-Deab and T. Ohsaka *J. Electrochem. Soc.* 155 (2005) D14.
3. M.M. Walczak, C.A. Alves, B.D. Lamp and M.D. Porter, *J. Electroanal. Chem.* 396 (1995) 103.
4. C.L. Perdriel and A.J. Arvia, M. Ipohorski, *J. Electroanal. Chem* 215 (1986) 317.
5. J.Gomez, L. Vasquez and A.M. Baro, C.L. Perdriel and A.J. Arvia, *Electrochim. Acta* 34 (1989) 619.
6. E. Higuchi, H. Uchida and M. Watanabe, *J. Electroanal. Chem.* 583 (2005) 69.
7. M.S. El-Deab and T. Ohsaka, *Electrochem. Commun.* 5 (2003) 214.
8. Md.R. Miah and T. Ohsaka, *J. Electroanal. Chem.* 533 (2009) 71.
9. Md.R. Miah and T. Ohsaka, *Electrochim. Acta* 52 (2007) 6378.
10. J.X. Wang, N.S. Marinkovic and R.R. Adzic, *Colloids and Surface* 134 (1998) 165.
11. R.R. Adzic and J.X. Wang, *Electrochim. Acta* 45 (2000) 4203.
12. R.R. Adzic and J.X. Wang, *Solid State Ionics*, 150 (2002) 105.
13. N.M. Markovic, H.A. Gasteiger, B.N. Grgur and P.N. Ross, *J. Electroanal. Chem.* 467 (1999)157
14. Md.R. Miah and T. Ohsaka, *Anal. Chem.* 78 (2006) 1200 and the references cited therein.
15. E.S Brandt, *J. Electroanal. Chem.* 150 (1983) 97.
16. C.C. Chang, S.L. Yau, J.W. Tu and J.S. Yang, *Surface Sci.* 523 (2003) 59.
17. C.A. Lucas, N.M. Markovic and P.N. Ross, *Surface Sci.* 340 (1995) L949.
18. R. Gómez, H.S. Yee, G.M. Bommarito, J.M. Feliu and H.D. Abruna, *Surface Sci.* 335 (1995) 101.

19. A.M. Bittner, J. Wintterlin, B. Beran and G. Ertl, *Surface Sci.* 335 (1995) 291.
20. D.D. Sneddon and A.A. Gewirth, *Surface Sci.* 343 (1995) 185.
21. T. Yamada, K. Ogaki, S. Okubo and K. Itaya, *Surface Sci.* 369 (1996) 321.
22. L.J. Wan and K. Itaya, *J. Electroanal. Chem.* 473 (1999) 10.
23. M. Kunitake, N. Batina, and K. Itaya, *Langmuir* 11 (1995) 2337.
24. N. Batina, M. Kunitake and K. Itaya, *J. Electroanal. Chem.* 405 (1996) 245.
25. A.T. Hubbard, *Chemical Rev.* 88 (1998) 633.
26. M.P. Soriaga, *Progress in Surface Sci.* 39 (1992) 325.
27. S. Sugita, T. Abe, and K. Itaya, *J. Phys. Chem.* 97 (1993) 8780.
28. J.L. Stickney, S.D. Rosaco, and A.T. Hubbard, *J. Electrochem. Soc.* 131 (1984) 260.
29. J. Hernández, J. Solla-Gullón and E. Herrero, *J. Electroanal. Chem.* 574 (2004) 185.
30. S.J. Hsieh and A.A. Gewirth, *Surface Sci.* 498 (2002) 147.
31. N. Batina, T. Yamada, and K. Itaya, *Langmuir* 11 (1995) 4568.
32. B.G. Bravo, S.L. Michelhaugh, M.P. Soriaga, I. Villegas, D. W. Suggs, and J.L. Stickney, *J. Phys. Chem.* 95 (1991) 5245.
33. P. Gao and M.J. Weaver, *J. Phys. Chem.* 90 (1986) 4057.
34. X. Gao and M.J. Weaver, *J. Am. Chem. Soc.* 114 (1992) 8544.
35. H. Matsumoto, J. Inukai and M. Ito, *J. Electroanal. Chem.* 379 (1994) 223.
36. N.J. Tao and S.M. Lindsay, *J. Phys. Chem.* 96 (1992) 5213.
37. X. Gao, G.J. Edens, and M.J. Weaver, *J. Phys. Chem.* 98 (1994) 8074.
38. W. Haiss, J.K. Sass, X. Gao and M.J. Weaver, *Surface Sci.* 274 (1992) L593.
39. R.L. McCarley and A.J. Bard, *J. Phys. Chem.* 95 (1991) 9618.
40. T. Yamada, N. Batina and K. Itaya, *Surface Sci.* 335 (1995) 204.
41. T. Yamada, N. Batina, and K. Itaya, *J. Phys. Chem.* 99 (1995) 8817.
42. U. Hasse and F. Scholz, *Electrochem. Commun.* 6 (2004) 409.
43. X.Z. Wu, B.M. Ocko, E.B. Sirota, S.K. Sinha and M. Deutsch, *Physica A* 200 (1993) 751.
44. B.M. Ocko, G.M. Watson, and J. Wang, *J. Phys. Chem.* 98 (1994) 897.
45. L. Han-Wei, H. Uchida and M. Watanabe, *J. Electroanal. Chem.* 413 (1996) 131.
46. Han-Wei Lei, H. Uchida, and M. Watanabe, *Langmuir* 13 (1997) 3523.
47. M.O. Finot, G.D. Braybrook, M.T. McDermott, *J. Electroanal. Chem.* 466 (1999) 234.
48. B.M. Ocko, O.M. Magnussen, X.J. Wang, R.R. Adzic and Th. Wandlowski, *Physica B* 221 (1996) 238.
49. A.Cuesta and D.M. Kolb, *Surface Sci.* 465 (2000) 310.
50. P. Broekmann, A. Spaenig, A. Hommes and K. Wandelt, *Surface Sci.* 517 (2002) 123.
51. Md.R. Miah, J. Masud and T. Ohsaka, *Electrochim. Acta* 54 (2008) 316.
52. Md.R. Miah, T.M. Alam and T. Ohsaka, *Anal. Chim. Acta* 669 (2010) 75.
53. A.Kongkanand and S. Kuwabata, *Electrochem. Commun.* 5 (2003) 133.
54. M.S. El-Deab, T. Ohsaka, *Electrochem. Commun.* 4 (2000) 288.
55. M.S. El-Deab, K. Arihara and T. Ohsaka, *J. Electrochem. Soc.* 151 (2004) E213.
56. A.Tadjeddine, A.L. Rille, *Electrochim. Acta* 45 (1999) 601.
57. X. Gao, G.J. Edens, F.-C. Liu, A. Hamelin and M.J. Weaver, *J. Phys. Chem.* 98 (1994) 8086.
58. N.M. Markovic, R.R. Adzic and V.B. Vesovic, *J. Electroanal. Chem.* 165 (1984) 121.
59. Md.R Miah and T. Ohsaka, *Electrochim. Acta* 54 (2009) 1570.
60. Md.R. Miah and T. Ohsaka, *J. Electrochem. Soc.* 153 (2006) E195.